

Investigation of plasma rotation in tokamaks heated by ICRF with a symmetrical k// spectrum

Y. Podoba¹, C. Angioni¹, R. Bilato¹, V. Bobkov¹, R.M. McDermott¹, V. Igochine¹,
J. -M. Noterdaeme^{1,2}, ASDEX Upgrade Team¹

¹Max-Planck-Institut für Plasmaphysik, EURATOM Association, Germany

²EESA Department, University Gent, Belgium

Introduction

Toroidal rotation in tokamak plasmas plays an important role in the transitions to improved confinement regimes, the formation of transport barriers and the suppression of resistive wall modes in tokamaks [1-3]. In large fusion devices, such as ITER, the external momentum input from neutral beam injection (NBI) is expected to be relatively small. Consequently, the investigation of other mechanisms responsible for driving the toroidal plasma rotation is a key research field for tokamak advanced scenarios. Intrinsic rotation drive mechanisms associated with ion cyclotron resonance frequency (ICRF) heating are of particular interest as intrinsic rotation in ICRF heated plasmas have been observed on multiple tokamak devices including, JET, DIII-D, Tore-Supra, ASDEX Upgrade (AUG), and C-Mod [4] and the observed behavior can not be completely reconciled with that observed in ohmic and electron cyclotron resonance heated (ECRH) plasmas.

In this work, the rotation in the ASDEX Upgrade (AUG) tokamak plasma in purely ICRF heated discharges is investigated. Although the direct external momentum due to ICRF heating is negligible because of the almost toroidally symmetric antenna spectrum, the short

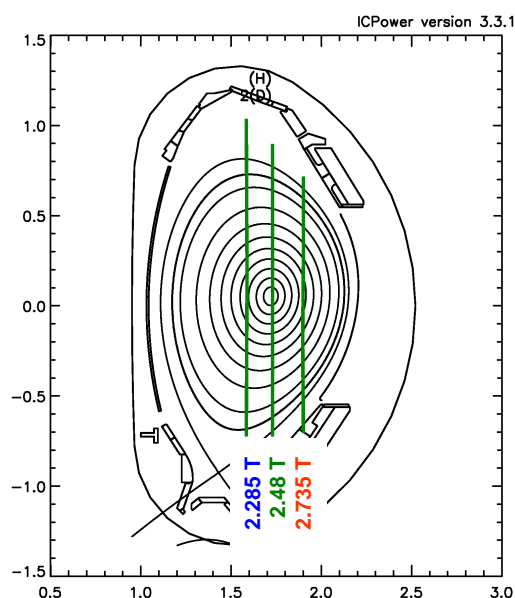


Fig.1. ASDEX Upgrade poloidal cross section with H (or 2nd D) resonance positions for $B_0 = 2.48, 2.285, \text{ and } 2.735\text{T}$

(16-20 ms) NBI blips, necessary for the charge-exchange-recombination spectroscopy (CXRS), can be a source of some external momentum. However, a backward extrapolation technique [5] allows for the determination of the true intrinsic rotation profiles.

It was shown previously [6] that the IC resonance location significantly influences the radial intrinsic plasma rotation profile. Three values of the toroidal magnetic field were tested: $B_0 = 2.48\text{T}$, which corresponds to a central H-resonance position and two off-axis cases $B_0 = 2.285\text{T}$ and 2.735T . The

positions of the resonances are shown schematically in figure 1. The measured rotation profiles for all three cases are shown in figure 3.

One of the possible mechanisms of establishing intrinsic rotation in the case of a symmetrical $k_{||}$ spectrum of the heating wave is the omnigenity breaking mechanism proposed by Chang [7,8]. According to this mechanism the trapped fast ion population can provide a counter-current contribution to the plasma rotation. Due to the radial excursion of the

resonant ions during the ICRF the net radial current, j_f , rises followed by a growth of the radial electric field E_r . The plasma responds by a return current, $j_p = -j_f$ which is equal in amplitude, but flows in the opposite direction. Both the resonant ions and the bulk plasma experience a toroidal $j \times B_\theta$ torque also equal in amplitude but oppositely directed ($j_p \times B_\theta = -j_f \times B_\theta$). Thus no net torque is obtained directly from the ICRF. Non-zero toroidal momentum comes from differences in the toroidal momentum loss rates for the resonant ions and the plasma. For a symmetrical $k_{||}$ spectrum the contributions of co-passing and counter passing ions cancel. Only a contribution from the trapped ions is considered in this mechanism.

Some features of the experimentally measured rotation profiles of AUG plasma are tentatively explained with this theory. However, one should keep in mind that the intrinsic rotation profiles are likely determined by multiple, and potentially competing, effects including not only ICRF related mechanisms but also core localized residual stress torques [9], convective contributions [10], and edge localized intrinsic rotation sources [11].

Calculations

In order to check the mechanism proposed by Chang a numerical simulation was done. For this purpose a simple single particle numerical model was built. In this model the guiding center trajectory of the ion is calculated by the Runge-Kutta method in a simple circular cross-section magnetic geometry. ICRF heating is simulated by a perpendicular energy kick obtained by the ion each time it passes the IC resonant layer. The average energy $\langle \delta W_\perp \rangle$ obtained by the particle at the resonant layer is estimated using the formula derived by Stix [12] and extended by Hammett [13].

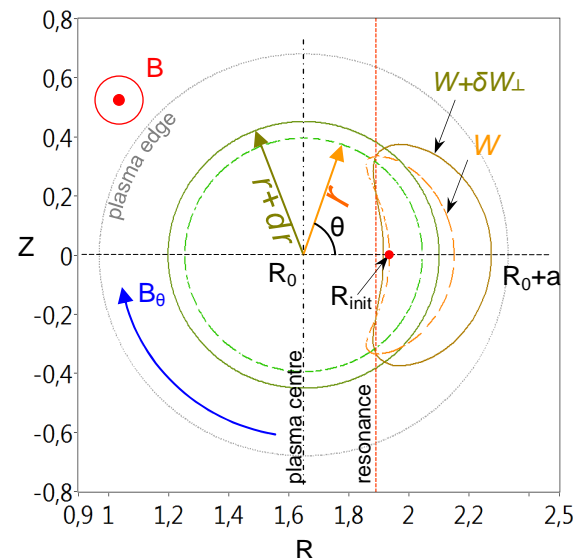


Fig.2. (color online) Change in the average radius r due to the ion's perpendicular energy increase.

The aim of the calculations is to estimate the force acting on the minority particles due to the omnigenity breaking mechanism. To this end, the radial current j_f caused by the modification of the banana orbits should be multiplied by the poloidal component of the magnetic field B_θ . The radial distribution of the force acting on the ions in the toroidal direction is obtained by doing so for each flux surface.

To estimate the radial current j_f it is necessary to know the average radial velocity $v_r = dr/\tau$ of the ion where τ is the bounce time and dr is the average radial displacement due to the ICRF heating (fig. 2). The last two values are calculated using the single particle model.

The initial position of the ion, R_{init} is varied radially from the centre $R_{init}=R_0$ to the outer edge of the plasma, $R_{init}=R_0+a$ in the equatorial plane with dR_{init} step. Thus, all flux surfaces are covered with the calculations. For each R_{init} the initial parallel and perpendicular (with respect to the magnetic field) velocities, $v_{||}$ and v_\perp , were varied in order to cover all possible combinations of the energy and pitch angle. The perpendicular energy kick $\langle \delta W_\perp \rangle$ is calculated for those ions whose trajectories intersect the IC resonant layer. By calculating the trajectory with the energy W and $W + \langle \delta W_\perp \rangle$ the radial velocity of the ion caused by the omnigenity breaking mechanism is found for each parallel and perpendicular velocity combination $v_r(v_{||}, v_\perp)$. (see fig.2). The velocity is convoluted with the distribution function $f(v_{||}, v_\perp)$ and multiplied by the minority density n_{min} , ions charge q and the volume enclosed between the magnetic surfaces passing through the points R_{init} and $R_{init}+dR_{init}$ for the corresponding flux surface. The minority-distribution function has been calculated with TORIC-SSFPQL package [14]. After integration over the $v_{||}$ and v_\perp the radially outward current j_f is obtained which is sustained by the fast ions. As was mentioned before, the plasma reacts on this current by an inward current $j_p = -j_f$ in order to conserve the plasma quasineutrality. Multiplying the plasma current j_p with the poloidal magnetic field component B_θ for a given flux surface the $j_p \times B_\theta$ ($J \times B$) force which is acting on the plasma layer in the toroidal direction is obtained. The $J \times B$ force times the major radius will give us the $J \times B$ torque. Due to the nature of this mechanism the resulting torque is always directed in the counter direction to the plasma toroidal current I_p .

It should be emphasized that the assumptions made in these calculations lead to an overestimation of the obtained value. However, the shape of the obtained radial profile gives the radial position where the effect is most pronounced. The magnitude of the effect can also be compared for the different resonance positions. Thus, in figure 3 the results of the

calculations are expressed in relative units and compared with the measured rotation profiles for three different cyclotron resonance positions.

Conclusions

From figure 3 it is clear that the position of the $J \times B$ maximum correlates with the behavior of the toroidal rotation. In the top case the $J \times B$ torque is largest outside of mid radius (and the resonance position) where a minimum in the rotation profile is observed. In the second case, with an on-axis ICRF resonance position, an almost equally large $J \times B$ torque is observed localized at $R=1.87$ m. Here, the edge rotation is much higher than in case (a) while a negative rotation gradient develops around the $J \times B$ peak resulting in a hollow rotation profile. For case (c) the relative magnitude of the $J \times B$ torque was

found to be smaller than in cases (a) and (b). The reason for this is that fewer particles are involved in the omnigenity breaking mechanism and only a small part of the marginally trapped particles reach the resonance layer at the HFS of the torus. The smaller predicted magnitude can explain the absence of an observable effect in the measured profile.

Despite the fact that the calculations are simplified and do not provide absolute values for the predicted torques, the correlations in radial position and magnitude demonstrate that omnigenity braking is potentially important for understanding and predicting intrinsic toroidal rotation profiles. More precise calculations should be done in order to estimate the omnigenity breaking mechanism not only qualitatively but also quantitatively.

References

- [1] Hahm T.S. 1994 Phys. Plasmas, 1 2940.
- [2] Terry P.W. 2000 Rev. Mod. Phys. 72 109.
- [3] Strait E.J. et.al. 1994 PRL 74, 2483.
- [4] J.E. Rice, et.al. Nucl. Fusion 47 (2007) 1618.
- [5] R M McDermott et al 2011 PPCF 53 124013.
- [6] Y. Podoba et.al. 38th EPS/ICPP, 2011, P4.092.
- [7] Chang et.al. Phys. Plasmas, V6, No.5 1969, (1999).
- [8] Chang et.al. Phys. Plasmas, V7, No.4 1089 (2000).
- [9] C. Angioni, et.al. PRL 107, 215003 (2011).
- [10] T. Tala, et.al. PRL 102, 075001 (2009).
- [11] J. Rice, et.al. PRL 106, 215001 (2011).
- [12] T.H. Stix, Nucl. Fusion 15 737 (1975).
- [13] G.W. Hammett dissertation thesis (1986).
- [14] R. Bilato, M. Brambilla et al., Nucl. Fus. Vol 51, p1030304 (2011).

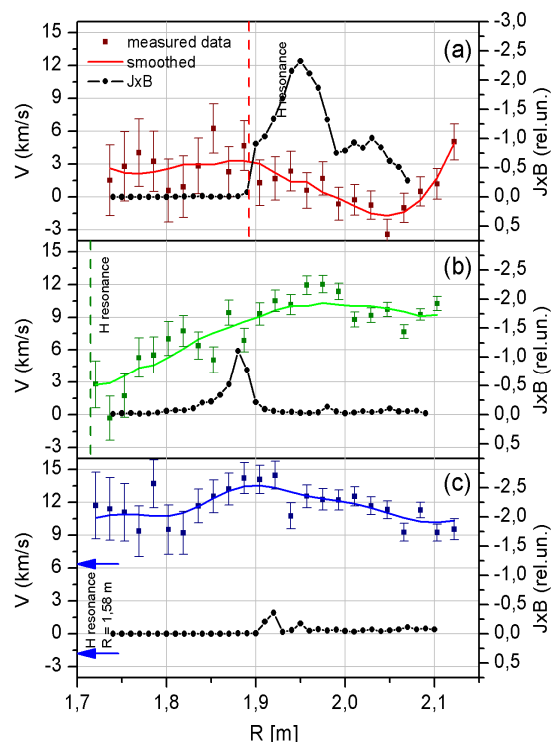


Fig. 3. Comparison of measured toroidal rotation with calculation results.

- a) $B_0=2.735$ T off-axis low field side #26621,
- b) $B_0=2.48$ T on-axis #26620,
- c) $B_0=2.285$ T off-axis high field side #26622.